

Mode-Specific Vibrational Energy Relaxation of Amide I' and II' Modes in N-Methylacetamide/Water Clusters: Intra- and Intermolecular Energy Transfer Mechanisms

Yong Zhang,[†] Hiroshi Fujisaki,[‡] and John E. Straub*

Department of Chemistry, Boston University, Boston, Massachusetts 02215

Received: December 13, 2008; Revised Manuscript Received: February 2, 2009

The mode-specific vibrational energy relaxation of the amide I' and amide II' modes in NMA- d_1 /(D₂O)_{*n*} (*n* = 0–3) clusters were studied using the time-dependent perturbation theory at the B3LYP/aug-cc-pvdz level. The amide modes were identified for each cluster based on the potential energy distribution of each mode. The vibrational population relaxation time constants were derived for the amide I' and II' modes. Results for the amide I' mode relaxation of NMA- d_1 /(D₂O)₃ agree well with previous experimental results. The energy relaxation pathways were identified, and both intra- and intermolecular mechanisms were found to be important. The amide II' mode was identified in the energy transfer pathways from the excited amide I' mode of NMA- d_1 /(D₂O)_{*n*} (*n* = 1–3) clusters. The modes associated with methyl group deformation were found to play a role in the mechanism of energy transfer from both excited amide I' and II' modes. The kinetics of energy flow in the cluster were examined by solving a master equation describing the vibrational energy relaxation process from excited system mode as a multistep reaction with the third order Fermi resonance parameters as the reaction rate constants. The intramolecular energy transfer mechanism was found to dominate the short time energy flow dynamics, whereas the intermolecular mechanism was found to be dominant at longer times.

1. Introduction

Vibrational energy relaxation (VER) is a fundamental process essential to the relationship between protein structure and function. While this topic has been intensely studied for decades,^{1–34} fundamental questions related to the mechanism of vibrational energy flow and dynamics in molecular systems remain. Recent advances in theoretical and computational methods now allow for the direct interpretation of state-of-the-art experimental studies of vibrational dynamics at the mode-specific level.^{35–37}

Amide I modes, mainly the localized C=O stretching motions of the protein backbone, have long been used as probes of protein secondary structure.^{38–41} Amide I modes are also known to play an important role in the energy transfer process in proteins following various reactions.⁴² The vibrational energy relaxation of the amide I mode in proteins has been studied,^{43,44} and vibrational relaxation time constants on the order of 1 ps have been reported for proteins with varying composition of α -helix and β -sheet structures, suggesting that the amide I mode relaxation time scale is independent of the protein secondary structure. In contrast, Fujisaki and Straub studied the vibrational relaxation of isotope labeled amide I modes in cytochrome *c*⁴⁵ and found that amide I bonds more exposed to solvent have faster relaxation rates with varying relative contributions of protein and water to the VER mechanism. These latter results indicate a sensitivity of the time scale and mechanism of the VER process to details of the surrounding environment. The exact role of intra- versus intermolecular energy transfer in

controlling the time scale and mechanism of VER in amide I mode in proteins remains an open question.

N-Methylacetamide (NMA) has the fundamental peptide bond structure of the protein backbone and has been widely used as a model for understanding the properties of proteins.^{46–55} The vibrational energy relaxation of the amide I mode has been studied employing a variety of methods.^{36,43,46,56} Using femto-second two-dimensional pump–probe spectroscopy (2D-IR), Hochstrasser and co-workers observed the vibrational relaxation time constant of the amide I' mode of NMA- d_1 (N–H to N–D deuterated NMA) to be 0.45 ps.⁴³ The authors suggested that the relaxation is dominated by intramolecular energy redistribution, arguing that the time scale is too fast to involve intermolecular energy transfer to the solvent (which generally occurs on a longer time scale).⁵⁷ They postulated that there may be energy transfer pathways with specific Fermi resonances and possible energy accepting modes including amide III', IV', and a NMA backbone C–C–N–C stretching motion (BS'). The strong coupling between amide I' and II' modes was reported in later experimental studies on several isotopically substituted forms of NMA by Tokmakoff and co-workers.⁵⁸ Ultrafast subpicosecond relaxation from the amide I mode was observed, and the relaxation was suggested to start by the exchange of energy between amide I, amide II, and other peptide modes, followed by slower dissipation to the bath. It was suggested that the amide III mode may serve as the dominant energy accepting mode from the excited amide I or II modes.

Energy transfer between the amide I' and II' modes of NMA- d_1 was simulated theoretically recently by Knoester and co-workers.^{59,60} By consideration of the energy dissipation to the amide II' mode only, the vibrational energy relaxation time constant for the amide I' mode was found to be 0.79 ps.⁶⁰ This result is close to the experimentally determined results of 0.45

* Corresponding author. E-mail: straub@bu.edu.

[†] Current address: Chemistry Department, University of Utah, Salt Lake City, UT 84112. E-mail address: zhangy@hec.utah.edu.

[‡] Current address: Integrated Simulation of Living Matter Group, Computational Science Research Program, RIKEN, Japan.

ps for the same system,^{43,46} indicating that energy transfer between the two modes forms an efficient energy transfer pathway from the excited amide I' mode. Opposite results were also reported, however, in which it was found that the amide I' mode weakly couples with internal NMA modes and direct energy transfer to the solvent is possible.³⁶

In this study, we applied the non-Markovian time-dependent perturbation theory⁶¹ with density functional theory level calculations to explore mode-specific energy transfer properties of NMA/water clusters in order to explore the time scale and mode-specific mechanism of the energy transfer process. All the bath modes were explicitly considered. Our theoretical models lead to physically reasonable predictions of the relaxation time scales and indicate that both intra- and intermolecular energy transfer mechanisms are essential to the mechanism of amide I' and II' mode vibrational relaxation.

2. Theory and Methods

2.1. Non-Markovian Time-Dependent Perturbation Theory.

The vibrational energy relaxation rate formula⁶¹ employed in this work is briefly summarized here. We expand the potential energy surface with respect to the normal coordinates of the system, q_S , and bath, q_α , and their frequencies, ω_S and ω_α , up to third and fourth order nonlinear coupling

$$H = H_S + H_B - q_S \delta F + q_S^2 \delta G \quad (1)$$

$$H_S = \frac{p_S^2}{2} + V(q_S) \quad (2)$$

$$H_B = \sum \left(\frac{p_\alpha^2}{2} + \frac{\omega_\alpha^2 q_\alpha^2}{2} \right) \quad (3)$$

$$\delta F = \sum_{\alpha,\beta} C_{S\alpha\beta} (q_\alpha q_\beta - \langle q_\alpha q_\beta \rangle) \quad (4)$$

$$\delta G = \sum_{\alpha,\beta} C_{SS\alpha\beta} (q_\alpha q_\beta - \langle q_\alpha q_\beta \rangle) + \sum_\alpha C_{SS\alpha} q_\alpha \quad (5)$$

where H_S (H_B) is the system (bath) Hamiltonian and $C_{S\alpha\beta}$ ($C_{SS\alpha\beta}$) are the third (fourth) order coupling terms. From the von Neumann–Liouville equation, a reduced density matrix for the system mode is derived using the time-dependent perturbation theory after tracing over the bath degrees of freedom. The commonly employed Markov approximation, which assumes a separation in time scales for the relaxation of the system and bath modes, is not invoked in this theory. The final VER formula is obtained as⁶¹

$$\begin{aligned} (\rho_S)_{00}(t) \approx & \frac{2}{\hbar^2} \sum_{\alpha,\beta} [C_{--}^{\alpha\beta} u_t(\tilde{\omega}_S - \omega_\alpha - \omega_\beta) + C_{+-}^{\alpha\beta} u_t(\tilde{\omega}_S + \\ & \omega_\alpha + \omega_\beta) + C_{+}^{\alpha\beta} u_t(\tilde{\omega}_S - \omega_\alpha + \omega_\beta)] \\ & + \frac{2}{\hbar^2} \sum_\alpha [C_{-}^{\alpha} u_t(\tilde{\omega}_S - \omega_\alpha) + C_{+}^{\alpha} u_t(\tilde{\omega}_S + \omega_\alpha)] \quad (6) \end{aligned}$$

where the subscript of $(\rho_S)_{00}$ indicates the vibrational ground state and $u_t(\Omega)$ is defined as

$$u_t(\Omega) = \int_0^t dt' \int_0^{t'} dt'' \cos \Omega(t' - t'') = \frac{1 - \cos \Omega t}{\Omega^2} \quad (7)$$

The coefficients, $C_{--}^{\alpha\beta}$, $C_{+-}^{\alpha\beta}$, $C_{+}^{\alpha\beta}$, C_{-}^{α} , and C_{+}^{α} , can be derived from the nonlinear coupling constants $C_{S\alpha\beta}$ and $C_{SS\alpha\beta}$ as⁶¹

$$\mathbf{C}^{\alpha\beta} = \begin{pmatrix} C_{--}^{\alpha\beta} & C_{+-}^{\alpha\beta} \\ C_{+-}^{\alpha\beta} & C_{++}^{\alpha\beta} \end{pmatrix} = \{(q_S)_{10} C_{S\alpha\beta} - (q_S^2)_{10} C_{SS\alpha\beta}\}^2 \mathbf{S}^{\alpha\beta} \quad (8)$$

$$\mathbf{S}^{\alpha\beta} = \frac{\hbar^2}{2\omega_\alpha \omega_\beta} \begin{pmatrix} (1+n_\alpha)(1+n_\beta) & 2(1+n_\alpha)n_\beta \\ 2(1+n_\alpha)n_\beta & n_\alpha n_\beta \end{pmatrix} \quad (9)$$

$$\mathbf{C}^\alpha = \begin{pmatrix} C_{-}^{\alpha} \\ C_{+}^{\alpha} \end{pmatrix} = (q_S^2)_{10} C_{SS\alpha}^2 \mathbf{R}^\alpha \quad (10)$$

$$\mathbf{R}^\alpha = \frac{\hbar}{2\omega_\alpha} \begin{pmatrix} 1+n_\alpha \\ n_\alpha \end{pmatrix} \quad (11)$$

where $n_\alpha = 1/(e^{\beta\hbar\omega_\alpha} - 1)$ is the thermal phonon number. When the system mode is excited to the $\nu = 1$ state, VER is described by the decay of the reduced density matrix element written most simply as $\rho_{11}(t) = 1 - \rho_{00}(t) \approx \exp[-\rho_{00}(t)]$ under the cumulant approximation. Following complete VER, it is possible that partial or complete dissociation of the system may occur. However, our study focuses on only the initial step in that VER process.

2.2. Simulation Protocol. We simulated *trans-N*-methylacetamide (NMA) in vacuum and in water cluster environments. The water molecules were placed around and about NMA forming hydrogen bonds (HBs) with the C=O oxygen and/or N–H hydrogen, similar to structures proposed in previous studies.^{62–64} We expect that the HBs between methyl hydrogen and water are much weaker,^{65,66} and such weak HBs were not considered to be important in this work. Up to three water molecules were involved, a small cluster but one reported previously to represent the most essential aspects of the solvation effect.^{48,65,67}

In order to mimic the electronic field due to bulk solvation, the NMA clusters with three water molecules were also studied with the polarizable continuum solvation model (PCM), using the integral equation formalism embedded in Gaussian 03.⁶⁸

This study is focused on deuterated NMA ($\text{CH}_3\text{-CO-ND-CH}_3$, NMA-*d*₁, instead of $\text{CH}_3\text{-CO-NH-CH}_3$, NMA-*h*₇) and its D₂O clusters, following previous experimental studies.^{43,46,58} Deuteration serves to eliminate the coupling between C=O stretching and water bending motions. Fully deuterated NMA-*d*₇ clusters were also studied in order to understand the role of the methyl groups in the VER process.

All calculations were carried out at the B3LYP/aug-cc-pvdz level using the Gaussian03 package.⁶⁸ The “verytight” SCF convergence criterion and “ultrafine” integration grid were applied in the calculation. The harmonic normal-mode analysis was carried out for the optimized structure. The third and fourth order anharmonic coupling constants were calculated using a finite difference method.⁶⁹

The system mode vibrational energy relaxation rate constants were derived by fitting the reduced density matrix $\rho_{11}(t)$ time

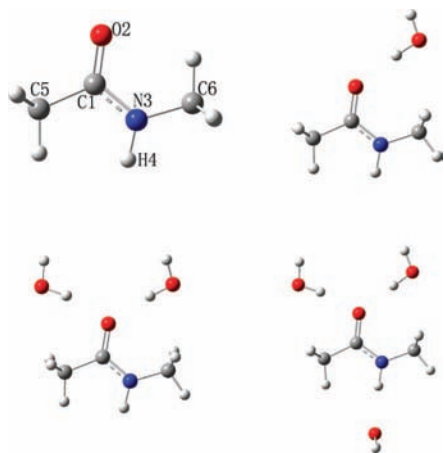


Figure 1. Depiction of the optimized structure of NMA/D₂O clusters at the B3LYP/aug-cc-pvdz level. The position of the solvent molecules in the NMA/(D₂O)₃ cluster with the PCM solvent model is similar to that without the PCM model (not shown here).

profiles. The energy transfer pathways were identified by calculating the third order Fermi resonance parameters defined as

$$r_{S\alpha\beta} = \frac{|C_{S\alpha\beta}|}{\hbar|\tilde{\omega}_S - \omega_\alpha - \omega_\beta|} \sqrt{\frac{\hbar}{2\tilde{\omega}_S}} \sqrt{\frac{\hbar}{2\omega_\alpha}} \sqrt{\frac{\hbar}{2\omega_\beta}} \quad (12)$$

where $\tilde{\omega}_S$ and ω_α are the frequencies of system mode and bath mode, respectively.

3. Results and Discussions

3.1. Optimized Structure and Calculated Frequencies. The positions of the water molecules in the geometry optimized clusters are depicted in Figure 1. The geometry optimized structure of NMA-*d*₁/(D₂O)₃ with the PCM solvent model was found to be similar to that without PCM and is not shown here. The calculated structure of the isolated NMA molecule was found to be similar to that measured from gas phase electron diffraction.⁷⁰ For example, the calculated C=O bond length is 1.229 Å compared to 1.225 Å from experiment. Addition of water molecules to form hydrogen bonds with the NMA carboxyl oxygen caused the C=O bond to be stretched to 1.236 Å (one water) and 1.246 Å (two waters), respectively, indicating the weakening of the carboxyl bond. By adding a third water to form a hydrogen bond with the N–D hydrogen, the C=O bond was further weakened and extended to 1.249 Å. The N–D bond was similarly extended from 1.009 Å in the isolated NMA to 1.016 Å in NMA-*d*₁/(D₂O)₃. The application of the PCM force field shifted the bonds further to 1.256 Å for C=O and 1.023 Å for N–D bonds.

Normal-mode analysis was carried out for each optimized structure. With the normal-mode vectors from DFT calculations, the potential energy distribution (PED) of each mode was calculated using the MOLVIB facility in CHARMM.⁷¹ The internal coordinates follow Pulay's definitions.⁷² The amide modes I'–VI' and the NMA backbone stretching motion (BS') were identified for isolated NMA-*d*₁ and its clusters with three D₂O molecules (see Table 1).

The frequency of the amide I' modes for each cluster is summarized in Table 2. For the NMA-*d*₁, the amide I' frequency was found to be 1727.9 cm⁻¹, close to that observed in experiment (1717 cm⁻¹).⁷³ With three D₂O molecules hydrogen bonded, the amide I' frequency red-shifted to 1668.8 cm⁻¹ in

NMA-*d*₁/(D₂O)₃, consistent with the observation that the C=O bond is weakened. With the additional PCM force field, the frequency was further shifted to 1624.5 cm⁻¹ in NMA-*d*₁/(D₂O)₃/PCM, in good agreement with the experimental value of NMA-*d*₁ in D₂O solution of 1623–1626 cm⁻¹.^{67,74} At the same time, the frequency of the amide II' mode was found to be blue-shifted upon solvation as shown in Table 3, consistent with previous experimental observations.⁶⁷

The calculated anharmonic frequencies from the time-dependent perturbation theory are also provided in Tables 2 and 3. The anharmonicity of the amide I' mode was found to be largest in NMA-*d*₁/(D₂O)₁ (92.0 cm⁻¹) and smallest in NMA-*d*₁/(D₂O)₃/PCM (35.2 cm⁻¹), similar to previous calculations (42.7 cm⁻¹).⁴⁸

3.2. VER of the Amide I' Mode. Applying the time-dependent perturbation theory described above, the vibrational energy transfer time constant from the excited amide I' mode was derived for each cluster (see Table 2). The time evolution of the initially excited density matrix element is shown in Figure 2 (left column) for the isolated NMA-*d*₁ and the three D₂O clusters. The recurring behavior observed in some clusters is partly due to the small size of the clusters examined in this study.

Subpicosecond time scales were found for the VER of the amide I' mode in all clusters. The amide I' mode in isolated NMA-*d*₁ has the slowest relaxation rate with $T_1 = 0.78 \pm 0.02$ ps. Adding one, two, or three D₂O molecules adds degrees of freedom that may serve as vibrational energy accepting bath modes. The VER time constants of the amide I' mode in NMA-*d*₁/(D₂O)₃ clusters were found to be 0.48 and 0.67 ps with or without the PCM force field, respectively, in agreement with experimentally determined values of ~0.45 ps.^{43,46} Our calculations indicate that the addition of water molecules shortens the VER time for the amide I' mode.

The energy transfer pathways from the excited amide I' mode were identified for each cluster by calculating the third order Fermi resonance parameters $r_{S\alpha\beta}$ using eq 12. For isolated NMA-*d*₁, NMA-*d*₁/(D₂O)₃, and NMA-*d*₁/(D₂O)₃/PCM, the calculated third order Fermi resonance parameters $r_{S\alpha\beta}$ of the important VER pathways (defined as $r_{S\alpha\beta} \geq 0.03$) are depicted in Figure 3 (upper panel). The detailed values are provided in the Supporting Information.

For isolated NMA-*d*₁, amide III', VI', and the BS' modes were found to be the dominant energy accepting modes from the excited amide I' mode. The amide II' mode was not involved due to a poor frequency resonance. The coupling between the amide I' and amide II' modes has been reported previously⁵⁸ and the energy transfer between the two modes suggested.^{58–60} For the NMA-*d*₁/D₂O cluster with one, two, or three water molecules, with or without the PCM force field, the amide II' mode was found to participate in the important energy transfer pathways from the excited amide I' mode. The modes dressing the amide II' mode in these pathways consist of delocalized bendinglike motions involving NMA and water molecules (hydrogen bonded to C=O bond). However, there is little deformation within each molecule. The frequencies of these modes are on the order of 100 cm⁻¹ and fit the frequency gap between amide II' mode and amide I' mode following anharmonic corrections (see Table 2). Other amide modes are also found to be involved in the important energy transfer pathways. For the fully solvated NMA-*d*₁/(D₂O)₃ cluster, amide IV', V', and BS' are involved without PCM, and amide V' is involved when PCM is applied. The availabilities of the NMA amide modes and BS' mode of NMA-*d*₁ and NMA-*d*₁/(D₂O)₃/PCM in

TABLE 1: Calculated Amide Modes of NMA- d_1 , Isolated or “Solvated” by Three Water Molecules, without or with the Bulk Solvent PCM Correction

	mode no.	freq (cm ⁻¹)	PED ^a (%)
NMA- d_1			
amide I'	23	1727.9	CO s (83), C1N s (4)
amide II'	22	1503.9	Me6 d (49), C1N s (16), Me6 r (12), NH r (5)
amide III'	10	929.3	NH r (60), Me5 d (18), C1N s (12), NC6 s (4)
amide BS'	9	854.3	C1N s (29), CC s (16), Me6 r (16), NC6 s (11)
amide IV'	8	617.5	CO r (41), CC s (32), NH d (11), CO d (5), NC6 s (5)
amide VI'	7	608.5	CO b oop (86), Me5 r (18)
amide V'	5	345.1	NH b oop (92)
NMA- d_1 /(D ₂ O) ₃			
amide I'	44	1668.8	CO s (72), C1N s (13)
amide II'	43	1519.5	C1N s (34), CC s (11), NH r (10), CO s (8)
amide III'	28	978.0	NH r (55), Me5 r (22), C1N s (9), NC6 s (7)
amide BS'	27	878.2	C1N s (23), CC s (18), NC6 s (12), Mr6 r (11)
amide IV'	26	632.3	CO r (42), CC s (31), NH d (10), NC6 s (5)
amide VI'	25	626.3	CO b oop (81), Me5 r (17)
amide V'	24	515.4	NH b oop (75), H2O b (19), H2O t (19)
NMA- d_1 /(D ₂ O) ₃ /PCM			
amide I'	44	1624.5	CO s (59), C1N s (22)
amide II'	43	1522.4	C1N s (31), CO s (18), CC s (13), NH r (12)
amide III'	28	996.4	NH r (39), Me5 r (38), C1N s (7)
amide BS'	27	881.4	C1N s (22), CC s (18), NC6 s (12), Me6 r (10)
amide IV'/VI'	26	632.9	CO b oop (38), CO r (19), CC s (14), Me5 r (7)
amide IV'/VI'	25	631.4	CO b oop (32), CO r (21), CC s (16), Me5 r (6)
amide V'	24	581.4	NH b oop (59), H2O t (14), H2O b (9)

^a The potential energy distribution was calculated using normal vectors computed at the B3LYP/aug-cc-pvdz level and using the MOLVIB facility in CHARMM.⁷¹ Small contributions (<4%) are ignored. Internal coordinates follow Pulay's definitions.⁷² Motions are defined as s = stretch, d = deformation, r = rock, b = bend, t = torsion, oop = out-of-plane. Atom indices (see Figure 1 for definition) are added when necessary, and Me stands for the methyl group. (Me5 is the methyl group containing C5.)

TABLE 2: Calculated Harmonic Frequencies, Corrected Anharmonic Frequencies, and VER Time Constants of the Amide I' Modes of the NMA/D₂O Clusters

cluster	harm freq (cm ⁻¹)	anharm freq (cm ⁻¹)	T_1 (ps)
NMA- d_1	1727.9	1679.0	0.78 ± 0.02
NMA- d_1 /(D ₂ O) ₁	1704.0	1612.0	0.67 ± 0.08
NMA- d_1 /(D ₂ O) ₂	1676.2	1591.4	0.56 ± 0.05
NMA- d_1 /(D ₂ O) ₃	1668.8	1580.1	0.48 ± 0.05
NMA- d_1 /(D ₂ O) ₃ /PCM	1624.5	1589.3	0.67 ± 0.03
NMA- d_7	1722.0	1665.1	0.93 ± 0.02
NMA- d_7 /(D ₂ O) ₃	1658.2	1560.4	0.67 ± 0.07
NMA- d_7 /(D ₂ O) ₃ /PCM	1608.7	1562.4	0.71 ± 0.03
exptl	1717 ^a		0.45 ^b
	1623 ^c		
	1626 ^d		

^a Data for NMA- d_1 in the gas phase.⁷³ ^b Data for NMA- d_1 in D₂O solution.⁴³ ^c Data for NMA- d_1 in D₂O solution.⁶⁷ ^d Data for NMA- d_1 in D₂O solution.⁷⁴

the important energy transfer pathways are summarized in Figure 4. The third order Fermi resonance parameters of all pathways are smaller than 0.40, small relative to those found in prior studies of mode-specific VER in porphyrin models.^{35,75,76}

3.3. VER of the Amide II' Mode. Similarly to those for the amide I' mode, the VER time scales from the excited amide II' modes were computed (see Table 3) and the important energy transfer pathways identified (see Figure 5 and the Supporting Information for details). The VER of the amide II' mode is predicted to have a subpicosecond relaxation time scale (with the exception of NMA- d_1 /(D₂O)₁ which has $T_1 = 1.03$ ps), which is somewhat slower than that of the corresponding amide I' mode in each cluster. With the addition of one, two, or three water molecules, the VER rate increases. The amide II' mode of NMA- d_1 /(D₂O)₃ cluster is predicted to have a VER time constant of

TABLE 3: Calculated Harmonic Frequencies, Corrected Anharmonic Frequencies, and VER Time Constants of the Amide II' Modes of the NMA/D₂O Clusters

cluster	harm freq (cm ⁻¹)	anharm freq (cm ⁻¹)	T_1 (ps)
NMA- d_1	1503.9	1588.4	0.81 ± 0.35
NMA- d_1 /(D ₂ O) ₁	1502.3	1518.5	1.03 ± 0.19
NMA- d_1 /(D ₂ O) ₂	1513.7	1500.8	0.88 ± 0.12
NMA- d_1 /(D ₂ O) ₃	1519.5	1444.5	0.75 ± 0.25
NMA- d_1 /(D ₂ O) ₃ /PCM	1522.5	1500.7	0.82 ± 0.05
NMA- d_7	1445.3	1427.7	0.89 ± 0.03
NMA- d_7 /(D ₂ O) ₃	1499.6	1407.3	0.75 ± 0.26
NMA- d_7 /(D ₂ O) ₃ /PCM	1511.0	1488.6	0.81 ± 0.04

0.75 ± 0.25 ps without the PCM force field and 0.82 ± 0.05 ps in the presence of the PCM force field.

For the excited amide II' mode of the isolated NMA- d_1 , the amide III', IV', and the BS' modes were involved in the important VER pathways (see Figure 4). (The amide III' and BS' modes were also found to be important to the VER from the excited amide I' mode.) For the excited amide II' mode of NMA- d_1 /(D₂O)₃ with or without the PCM force field, the BS' mode and the amide IV' and VI' modes were involved in the important VER pathways. The BS' and amide IV' modes were found to be common for the energy relaxation from the excited amide I' and II' modes of the cluster without the PCM force field.

3.4. Role of Methyl Groups in VER. NMA is a small molecule having 12 atoms, 8 of which belong to the two terminal methyl groups (denoted as Me5 and Me6, respectively; see Figure 1). In addition to the amide modes and the BS motion, which are mainly associated with the peptide bond (O=C-N-D) atoms, the two methyl groups are also involved in the VER from the excited amide I' and II' modes. For example, mode 17 in the isolated NMA- d_1 with frequency 1411.5 cm⁻¹ forms

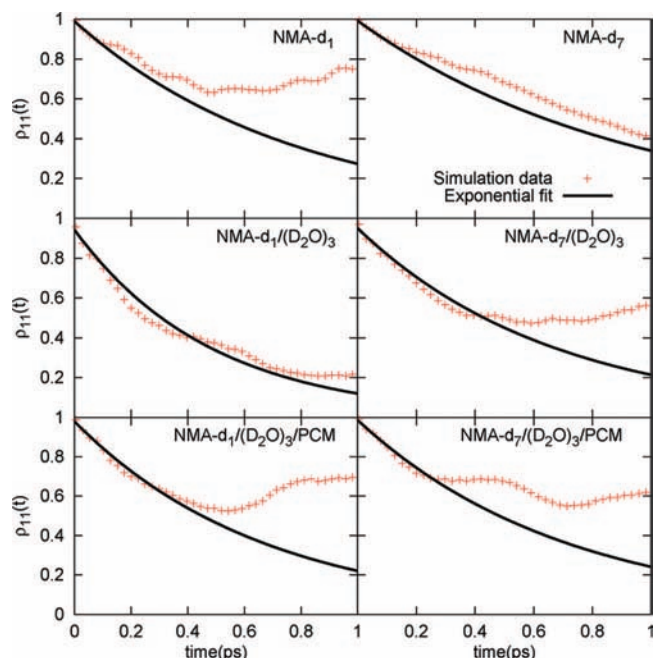


Figure 2. Time evolution of the initially excited density matrix element ρ_{11} for the amide I' mode of isolated NMA- d_1 and NMA- d_1 /(D₂O)₃ clusters (left column) and isolated NMA- d_7 and NMA- d_7 /(D₂O)₃ clusters (right column). The simulation data are shown as points, and the single exponential fit to the initial decay is shown as a solid line. The fitted time constants are summarized in Table 2. For each cluster, the calculated third order Fermi resonance parameters of the important VER pathways are plotted in Figure 3.

the most important VER pathway (with the largest third order Fermi resonance parameter) with mode 4 from the excited amide I' mode. That single mode is predicted from PED analysis to have 74% contribution from the Me6 deformation motions, whereas mode 12 with frequency 1035.6 cm⁻¹, involved in the second most important VER pathway for the excited amide I' mode, is predicted to have 70% contribution from Me5 deformation. Similar methyl group deformation motions with frequencies 1000–1100 cm⁻¹ (modes 29–32) or 1400–1500 cm⁻¹ (mode 38–42) were identified in the most important VER pathways for the excited amide I' modes of NMA- d_1 /(D₂O)₃

clusters (see Figure 3). These methyl motions were also involved in the VER pathways for the excited amide II' modes (see Figure 5)

To have a better understanding of the role of the methyl groups in the VER process, the fully deuterated NMA- d_7 and its clusters with three D₂O molecules were studied. The identified amide modes are summarized in Table 4. The derived VER time scales for the excited amide I' modes and amide II' modes are summarized in Tables 2 and 3, respectively. The important VER pathways were identified and the third order Fermi resonance parameters plotted in Figure 3 (lower panel) and Figure 5 (lower panel), respectively. The detailed values are included in the Supporting Information.

Upon deuteration of the methyl groups, the frequencies of the amide I' mode were red-shifted by ~ 6 cm⁻¹ for the isolated NMA and ~ 10 cm⁻¹ (~ 16 cm⁻¹) for the three water clusters without (with) PCM force field. The red-shift for the amide II' mode is more significant for the isolated NMA (>50 cm⁻¹). The shift is computed to be ~ 20 cm⁻¹ for the three water cluster without PCM force field, and ~ 11 cm⁻¹ with PCM applied, similar to the three water clusters of NMA- d_1 . Frequencies of other modes are also affected (see Tables 1 and 4).

For the VER of the excited amide I' mode, it was found to be slower in the fully deuterated NMA- d_7 clusters (see Table 2), consistent with previous observations.³⁷ The VER of the excited amide II' mode is also slower in isolated NMA- d_7 than in NMA- d_1 , whereas its three water clusters have VER rates similar to the corresponding NMA- d_1 clusters (see Table 3). Due to the frequency shifts relative to NMA- d_1 complexes, the bath modes involved in the VER pathways of NMA- d_7 show differences. For the isolated NMA- d_7 , the amide II' mode as well as amides III', IV', and BS' are involved in the essential VER pathways (see Figure 4). The amide II' mode is found to combine with mode 4, associated with N–D and C=O deformation motions. Amide III', dressed by the BS' mode, forms the most important VER pathway for the excited amide I' mode. For the NMA- d_7 /(D₂O)₃ clusters, the amides II', IV' V', and BS' are involved in the important energy transfer pathways in the absence of the PCM force field, whereas amides V', VI', and BS' are involved when PCM is applied.

The frequencies of modes associated with methyl group deformation motions were shifted to 800–900 cm⁻¹ (modes

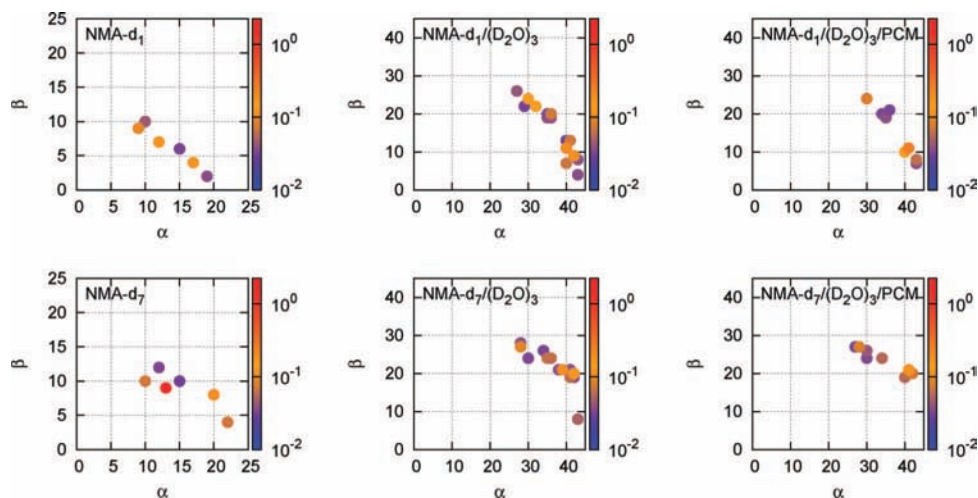


Figure 3. Calculated third order Fermi resonance parameters $r_{S\alpha\beta}$ of the important VER pathways (defined as $r_{S\alpha\beta} \geq 0.03$) for the amide I' mode in isolated NMA- d_1 and NMA- d_1 /(D₂O)₃ clusters (upper panel) and isolated NMA- d_7 and NMA- d_7 /(D₂O)₃ clusters (lower panel). (Detailed values are provided in the Supporting Information.) The x and y axes are the indices of the bath modes. The fitted time constants are summarized in Table 2.

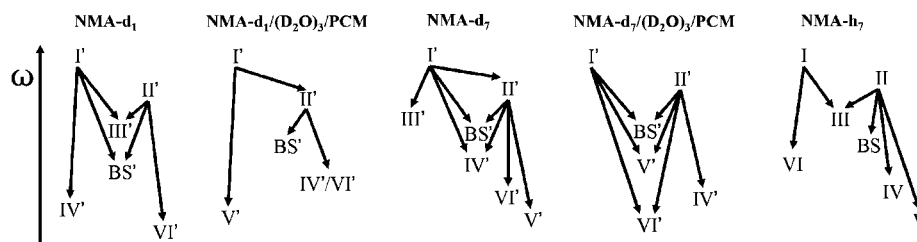


Figure 4. Graphic depiction of the energy transfer to the NMA amide modes and backbone stretching (BS) mode from the excited amide I' and II' modes of NMA-*d*₁, NMA-*d*₁/(D₂O)₃/PCM, NMA-*d*₇, and NMA-*d*₇/(D₂O)₃/PCM, and the amide I and II modes of NMA-*h*₇. Only those modes involved in the essential energy transfer pathways are included.

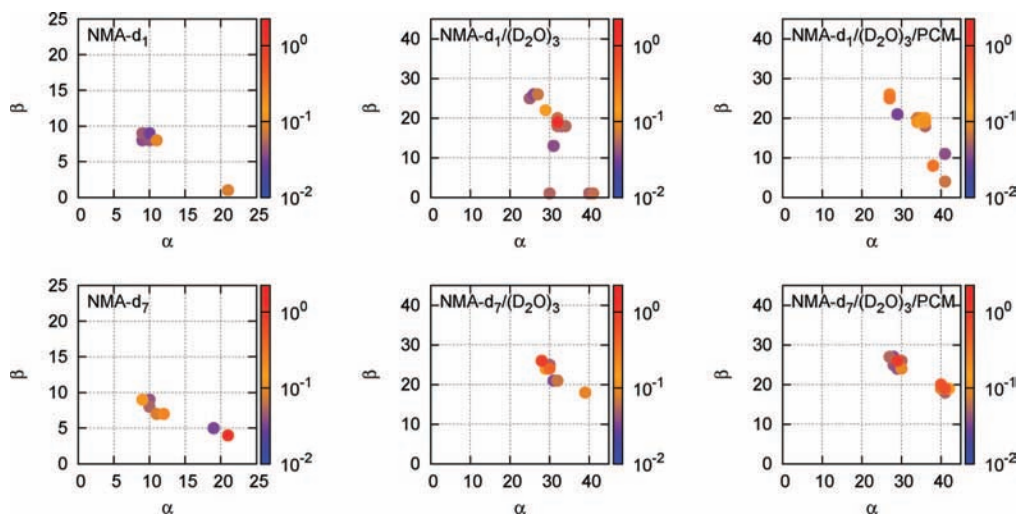


Figure 5. Calculated third order Fermi resonance parameters $r_{S\alpha\beta}$ of the essential VER pathways for the amide II' mode in isolated NMA-*d*₁ and NMA-*d*₁/(D₂O)₃ clusters (upper panel) and isolated NMA-*d*₇ and NMA-*d*₇/(D₂O)₃ clusters (lower panel). (Detailed values are provided in the Supporting Information.) The x and y axes are the indices of the bath modes. The fitted time constants are summarized in Table 3.

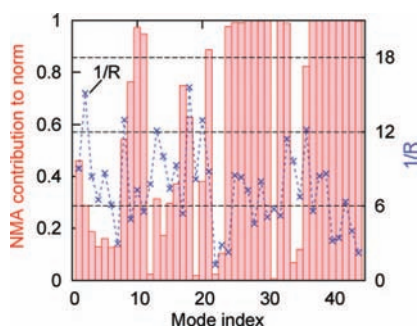


Figure 6. NMA contribution to the norm for each mode of NMA-*d*₁/(D₂O)₃/PCM (up to the amide I' mode, filled box) and the inverse participation ratio, $1/R$, of each mode (shown as points to the right axis). Both solute (NMA) and solvent (D₂O) motions are involved in the essential energy transfer pathways, and most accepting modes are predicted to be delocalized.

27–29 for the three water clusters) and 1000–1100 cm⁻¹ (modes 32–38 for the three water clusters). These methyl group deformation modes are still involved in the VER pathways for the excited amide I' modes but combine with different partners when compared to NMA-*d*₁ clusters. This indicates the essential role of these modes to the VER mechanism, whereas those modes dressing them serve to fit the frequency gap to satisfy the resonance condition. As energy accepting modes, the methyl groups in NMA-*d*₇ clusters are slightly less important relative to NMA-*d*₁ clusters, as indicated by slightly smaller third order Fermi resonance parameters for the pathways of NMA-*d*₇ clusters (see Figure 3). Similar properties were observed for both modes important to the VER mechanism for the excited amide II' modes.

For NMA-*d*₇/(D₂O)₃ clusters, with or without the PCM force field, the energy transfer rate of the excited amide I' mode is faster than that of the excited amide II' mode. This prediction is in qualitative agreement with the experimental results of Tokmakoff and co-workers.⁵⁸ In their study, the opposite trend was found for NMA-*h*₇ in DMSO where the VER rate is faster for the amide II mode primarily due to a slowing of the amide I mode VER. In an effort to explore the mechanism underlying this observation, the NMA-*h*₇ and its three H₂O clusters were studied in this work. The identified amide modes are summarized in Table 5. The amide I mode is found to couple with the H₂O bending motions in these complexes. In NMA-*h*₇/(H₂O)₃/PCM cluster, the amide I and II modes each split into two modes, labeled as 44 and 43 or 42 and 41, respectively. Due to this strong coupling, the predictions of the perturbation theory are unreliable. Direct calculations considering DMSO as the solvent may explain the surprising result that amide II mode relaxes faster than amide I mode.

3.5. Intra- and Intermolecular VER Mechanisms. In agreement with prior studies, our results indicate that intramolecular energy transfer plays an essential role in the vibrational energy relaxation of the amide I' and amide II' modes. The energy accepting modes include those associated with the O=C–N–D peptide bond as well as those associated with methyl group vibration.

Importantly, and in contrast to prior studies, our results indicate an important role for motions associated with water molecules in the mechanism of energy transfer. One example is the sub-100 cm⁻¹ mode dressing the amide II' motion and thereby assisting energy relaxation from the excited amide I' mode in NMA-*d*₁/D₂O clusters. In addition to PED, an alterna-

TABLE 4: Calculated Amide Modes of NMA-*d*₇, Isolated or “Solvated” by Three Water Molecules, without or with the Bulk Solvent PCM Correction

	mode no.	freq (cm ⁻¹)	PED ^a (%)
NMA- <i>d</i> ₇			
amide I'	23	1722.0	CO s (85), CO d (4), C1N s (4)
amide II'	22	1445.3	C1N s (50), NH r (15), NC6 s (12), CC s (9), CO r (9)
amide III'	13	932.8	NH r (33), NC6 s (20), Me5 d (10), Me6 d (10)
amide BS'	9	731.5	Me6 r (35), C1N s (22), Me5 r (16), NC6 s (7), CC s (6)
amide IV'	8	563.3	CO r (37), CC s (30), CO d (6)
amide VI'	7	536.0	CO b oop (61), Me5 r (38)
amide V'	5	339.3	NH b oop (91)
NMA- <i>d</i> ₇ /(D ₂ O) ₃			
amide I'	44	1658.2	CO s (78), C1N s (11), CO d (4)
amide II'	43	1499.6	C1N s (50), NH r (14), CC s (12), CO r (9), NC6 s (9)
amide III'	31	954.0	NC6 s (26), NH r (22), Me5 d (14), Me6 d (11), CC s (8)
amide BS'	27	753.2	Me6 r (37), C1N s (17), Me5 r (16), NC6 s (9), CC s (5)
amide IV'	26	580.3	CO r (36), CC s (30), NH d (5), CO d (5)
amide VI'	25	559.9	CO b oop (44), Me5 r (26), NH b oop (16)
amide V'	24	502.7	Nh b oop (56), H2O b (29), Me5 r (13)
NMA- <i>d</i> ₇ /(D ₂ O) ₃ /PCM			
amide I'	44	1608.7	CO s (70), C1N s (19), CO d (4)
amide II'	43	1511.0	C1N s (44), NH r (14), CC s (13), CO s (9), CO r (8)
amide III'	31	959.1	NC1 s (25), Me5 d (18), NH r (15), Me6 d (14), CC s (7)
amide BS'	27	755.6	Me6 r (36), Me5 r (17), C1N s (16), CO r (8), NC1 s (8)
amide V'	26	601.7	NH b oop (54), H2O t (20), CO b oop (11), H2O b (10)
amide IV'	25	580.0	CO r (35), CC s (29), CO d (6), NC1 s (5), NH d (5)
amide VI'	24	532.4	CO b oop (43), Me5 r (34), NH b oop (11), Me5 t (4)

^a See notes in Table 1.**TABLE 5: Calculated Amide Modes of NMA-*h*₇, Isolated or “Solvated” by Three Water Molecules, without or with the Bulk Solvent PCM Correction**

	mode no.	freq (cm ⁻¹)	PED ^a (%)
NMA- <i>h</i> ₇			
amide I	23	1732.5	CO s (81), CO d (4)
amide II	22	1560.3	NH r (45), C1N s (23), Me6 r (11), NC6 s (5)
amide III	15	1265.4	C1N s (28), NH r (28), CC s (9), CO r (8), Me5 d (6)
amide BS	10	988.2	Me5 r (56), CC s (21), NC6 s (7), CO s (4)
amide VI	8	627.4	CO b oop (79), Me5 r (15), NH b oop (6)
amide IV	7	621.0	CO r (40), CC s (33), NH d (10), NC6 s (6)
amide V	6	456.1	NH b oop (79), Me6 t (16), Me5 r (3)
NMA- <i>h</i> ₇ /(H ₂ O) ₃			
amide I	44	1679.3	CO s (49), HOH b (27), C1N s (7)
amide II	40	1597.6	NH r (52), C1N s (28), CO r (5)
amide III	33	1324.2	NH r (27), C1N s (26), Me5 d (17), CC s (7), CO r (6)
amide BS	27	888.9	C1N s (24), CC s (17), Me6 r (16), NC6 s (9), CO r (8)
amide V	26	733.0	NH b oop (57), H2O t (18), H2O b (17), CO b oop (13)
amide IV	24	635.9	CC s (41), H2O b (28), CO r (27), NH d (10)
amide VI	22	600.5	CO b oop (57), OB b oop (13), Me5 r (13)
NMA- <i>h</i> ₇ /(H ₂ O) ₃ /PCM			
amide I	44	1637.3	HOH b (50), CO s (26), NH r (7)
	43	1631.7	NH r (34), HOH b (29), CO s (21)
amide II	42	1626.1	HOH b (60), C1N s (13), CO s (6), NH r (6)
	41	1614.8	HOH b (27), C1N s (23), NH r (17), CO s (9)
amide III	33	1341.3	Me5 d (30) C1N s (23), NH r (19), CO s (7), CC s (5)
amide BS	27	892.4	C1N s (22), CC s (18), Me6 r (12), NC6 s (9), CO r (8)
amide V	26	824.2	Nh b oop (59), H2O t (32)
amide IV	24	634.1	H2O b (72), CO r (39)
amide VI	22	612.2	CO b oop (69), H2O b (28)

^a See notes in Table 1.

tive quantitative measure, the norm contribution from the NMA molecule, L_{NMA} , was calculated for each mode of the NMA-*d*₇/(D₂O)₃/PCM cluster as shown in Figure 6 (up to the amide I' mode). A contribution of 1.0 (0.0) indicates the mode is localized in the NMA (water) molecule. Modes 40, 41, and 43, which are involved in key energy transfer pathways from the amide I' mode, are strongly localized in the NMA molecule,

whereas modes such as 7 and 8 are more delocalized and include significant contribution from water motions.

Direct energy transfer to the solvent is one possible reason that faster VER rates of the amide I' and II' modes are observed for clusters with increasing numbers of water molecules. Master equations have been used to study the vibrational energy flow process.^{75,77} By considering (1) the initially excited system mode

to be the reactant, (2) the VER process to be a multistep reaction, and (3) the third order Fermi resonance parameters to be proportional to the mode-to-mode energy flow rate constants, a coarse-grained picture of the VER kinetics was provided by solving a master equation for energy relaxation in the isolated NMA- d_1 and NMA- $d_1/(D_2O)_3/PCM$ cluster. Considering only the transfer of population from high frequency modes to low frequency modes $A \rightarrow B + C$ with frequencies $\omega_A > \omega_B$ and $\omega_A > \omega_C$, the master equation was defined as

$$\frac{\partial P}{\partial t} = RP \quad (13)$$

with P being the population of each mode and the rate coefficients approximated as

$$R_{ij} = \sum_k r_{jik} \quad \text{for } j > i \quad (14)$$

$$R_{ii} = - \sum_{j < i} \sum_{k \leq j} r_{ijk} \quad (15)$$

where r_{ijk} are the third order Fermi resonance parameters.

The third order Fermi resonance parameters r_{ijk} for each mode i were calculated from the harmonic frequencies and third order anharmonic coupling constants using eq 12. With the boundary condition $P(S) = 1$ and $P(\alpha) = 0$ at $t = 0$, eq 13 was solved for each cluster with the amide I' mode as reactant and the lowest frequency mode as the final product. The energy $E(i) = P(i) \times \hbar\omega(i)$ was calculated for each mode i at a given time t .

While not a true kinetic equation with a well defined time scale, this model provides insight into the overall mechanism of vibrational energy flow and the competition between intra- and intermolecular energy transfer. The relaxation of the amide I' modes are predicted to follow a single exponential decay with time constants of 0.866 (arbitrary time units) for the isolated NMA- d_1 and 0.262 for NMA- $d_1/(D_2O)_3/PCM$, respectively. The time evolution of the energy decay is shown in Figure 7 (top) together with the energy evolution of the amide modes and the BS' mode (middle and bottom panels, respectively). With D_2O molecules included in the clusters, the energy flow is more efficient in NMA- $d_1/(D_2O)_3/PCM$ than in the isolated NMA- d_1 . Results for NMA- $d_1/(D_2O)_3$ (not shown here) were found to be similar to NMA- $d_1/(D_2O)_3/PCM$.

The energy of each mode can be divided into two parts, the NMA molecule and the surrounding D_2O . We calculated the relative contributions to the energy relaxation due to each subsystem by summing the product of the energy, E_i , and norm contributions, L_i , of each mode i at a given time t , $E_{NMA}(t) = \sum_i E_i(t) \times L_{i,NMA}$ for the NMA molecule and $E_{D_2O}(t) = \sum_i E_i(t) \times L_{i,D_2O}$ for the water molecules, respectively, over all modes. For NMA- $d_1/(D_2O)_3/PCM$, the results are shown in Figure 8. The excited amide I' mode and all higher frequency modes are excluded from the summation. Note that the total energy is not conserved due to the inclusion of nonresonant energy transfer with significant frequency mismatch, in agreement with the predictions of the time-dependent perturbation theory.

The inset of Figure 8 provides the long time behavior of the energy distribution between NMA and the surrounding water molecules. For this small system, the "reaction" is complete after $t \sim 100$, and the final energy distribution is determined by the lowest frequency mode (mode 1), which is predicted to have a significant contribution from water molecules (see Figure

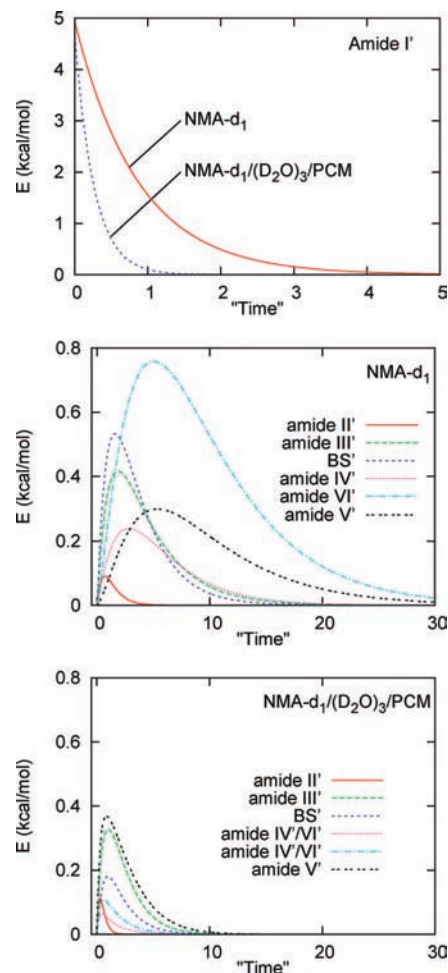


Figure 7. Evolution of energy flow from the initially excited amide I' mode calculated for the NMA- $d_1/(D_2O)_3/PCM$ cluster by solving a master equation. Top, relaxation of the amide I' mode; middle, evolution of the energy of the amide II'–VI' modes and the BS' mode of NMA- d_1 ; bottom, evolution of the energy of the amide II'–VI' modes and the BS' mode of NMA- $d_1/(D_2O)_3/PCM$. Results indicate that inclusion of solvent molecules in the cluster accelerates the energy transfer process. Similar behavior was observed for the VER process for the amide II' mode (not shown here).

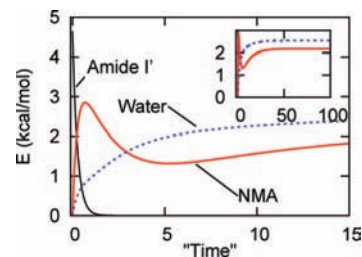


Figure 8. Evolution of the vibrational energy flow of the amide I' mode, the NMA molecule, and the water molecules calculated for the NMA- $d_1/(D_2O)_3/PCM$ cluster by solving a master equation model for the initially excited amide I' mode. The excited amide I' mode and all higher frequency modes are excluded from the energy calculated for the NMA molecule (see text for calculation details). The asymptotic behavior is shown in the inset. Initially, the energy flow is dominated by intramolecular mechanisms with intermolecular mechanisms playing a dominant role at longer times. Similar behavior was observed for the VER process for the amide II' mode (not shown here).

6). Note that this energy distribution is different from the ensemble averaged energy distribution of a system at thermal equilibrium. At short times, the energy of the accepting modes localized within the NMA molecule increases faster than the

energy of modes localized within the water molecules, indicating that the intramolecular energy transfer mechanism is dominant. From $t = 0.70$, the overall energy in the NMA molecule starts to decrease whereas the energy in the water molecules continues to increase, suggesting that the intermolecular energy transfer mechanism begins to dominate the energy transfer process. After $t \approx 3.0$, the water molecules have more energy than NMA. The same analysis was carried out for the excited amide II' mode, and similar results were obtained, indicating that energy first flows from the excited amide II' modes to accepting modes localized within NMA, followed by energy flow to the solvent.

The participation ratio is a measure of the delocalization of a normal mode⁷⁸ and defined as $R_i = \sum_j U_{ij}^4$, where U_{ij} represents the matrix of eigenvectors and the sum runs over all $3N$ degrees of freedom of the system with N atoms. The value of $1/R_i$ corresponds to the number of atoms participating in the i th mode. The computed $1/R_i$ values for the NMA- d_1 /(D₂O)₃/PCM cluster are plotted in Figure 6 as points. For most modes, $1/R$ has values larger than 6.0, 6 of which are larger than 12.0, including mode 8, which was found in the dominant energy transfer pathways for both the excited amide I' and II' modes. The contribution of both intra- and intermolecular energy transfer pathways and the delocalization of the bath modes results in efficient energy relaxation from the excited amide I' and II' modes.

4. Summary and Conclusions

We have provided a picture of mode-specific vibrational energy relaxation of the amide I' and amide II' modes in isolated NMA- d_1 and its hydrogen bonded D₂O clusters (up to three D₂O molecules) derived from time-dependent perturbation theory⁶¹ and quantum chemical calculation at the B3LYP/aug-cc-pvdz level. The polarizable continuum solvent model of water was applied to the NMA- d_1 /(D₂O)₃ cluster to mimic the electrostatic force field due to bulk solvation. The calculated harmonic frequencies of the amide I' mode, 1727.9 cm⁻¹ for NMA- d_1 and 1624.5 cm⁻¹ for NMA- d_1 /(D₂O)₃/PCM, respectively, agree well with the experimentally measured values (1717 cm⁻¹ for NMA- d_1 in gas phase⁷³ and 1623 cm⁻¹ for NMA- d_1 in D₂O solution),⁶⁷ and the solvation-induced shift in the amide I' mode frequency was reproduced in our calculations, supporting the accuracy of our treatment of the ground-state potential energy surface.

The energy transfer time constants were derived for the amide I' and II' modes in each cluster, and ultrafast subpicosecond time scales were obtained. The results for NMA- d_1 /(D₂O)₃ (0.48 ± 0.05 ps) and NMA- d_1 /(D₂O)₃/PCM (0.67 ± 0.03 ps) agree with the experimentally determined value of 0.45 ps.^{43,46} Energy relaxation from the excited amide II' modes was found to be slightly slower than the corresponding amide I' mode in each cluster.

The important energy transfer pathways from the excited amide I' and amide II' modes were identified for each cluster by calculating the third order Fermi resonance parameters. As indicated in eq 12, important energy transfer pathways are those having strong coupling (large $C_{S\alpha\beta}$) and good frequency match (small $|\omega_S - \omega_\alpha - \omega_\beta|$) with the excited system mode. The amide II' mode was not found to participate in the mechanism of energy transfer from the amide I' mode of the isolated NMA- d_1 . However, the amide II' mode was found to be involved in energy transfer from the amide I' mode of the NMA- d_1 /(D₂O)_{*n*} ($n = 1-3$) clusters when dressed by a low frequency (100 cm⁻¹) delocalized mode associated with the relative motion of the NMA and D₂O molecules. Other amide modes were found to

be involved in the energy transfer pathways from the excited amide I' and II' modes. Two groups of methyl deformation motions, having frequencies 1000–1100 and 1400–1500 cm⁻¹, were found to be important to the mechanism of energy transfer from the excited amide I' and II' modes.

In addition to intramolecular energy transfer mechanisms, intermolecular energy transfer to the solvating water molecules was also predicted to be important for the excited amide I' and II' modes. By solving an *ad hoc* master equation, modeling the VER process as a multistep reaction where the third order Fermi resonance parameters serve as approximate mode-to-mode energy flow rate constants, it was found that the energy flow in NMA is faster when it is hydrogen bonded to water molecules than in vacuum. This enhancement in the rate of energy flow results from direct energy transfer to the solvent molecules. This analysis combined with our more quantitative assessment of mode-specific energy transfer rates lead to an overall picture of energy transfer dominated by intramolecular energy transfer at short times with intermolecular energy transfer playing a dominant role at the longer times. Given the limitations of our theoretical model, the connection to experiments performed in bulk solvent is limited. Nevertheless, our study does provide insight into VER in isolated NMA and the effect of limited "solvation" on the VER process.

Acknowledgment. We are grateful for the generous support of this research by the National Science Foundation (Grants No. CHE-0316551 and CHE-0750309) and Boston University's Center for Computational Science.

Supporting Information Available: The coordinates of the optimized geometry structure of each cluster and the details of the important energy transfer pathways. This information is available free of charge via the Internet at <http://pubs.acs.org>.

References and Notes

- (1) Munck, E.; Champion, P. M. *Ann. N.Y. Acad. Sci.* **1975**, *244*, 142–162.
- (2) Sage, J. T.; Paxson, C.; Wyllie, G. R. A.; Sturhahn, W.; Durbin, S. M.; Champion, P. M.; Alp, E. E.; Scheidt, W. R. *J. Phys.: Condens. Matter* **2001**, *13*, 7707–7722.
- (3) Sage, J. T.; Durbin, S. M.; Sturhahn, W.; Wharton, D. C.; Champion, P. M.; Hession, P.; Sutter, J.; Alp, E. E. *Phys. Rev. Lett.* **2001**, *86*, 4966–4969.
- (4) Ye, X.; Demidov, A.; Rosca, F.; Wang, W.; Kumar, A.; Ionascu, D.; Zhu, L.; Barrick, D.; Wharton, D.; Champion, P. M. *J. Phys. Chem. A* **2003**, *107*, 8156–8165.
- (5) Henry, E. R.; Eaton, W. A.; Hochstrasser, R. M. *Proc. Natl. Acad. Sci. U.S.A.* **1986**, *83*, 8982–8986.
- (6) Henry, E. R.; Hochstrasser, R. M. *Proc. Natl. Acad. Sci. U.S.A.* **1987**, *84*, 6142–6146.
- (7) Elber, R.; Karplus, M. *Science* **1987**, *235*, 318–321.
- (8) Elber, R.; Karplus, M. *J. Am. Chem. Soc.* **1990**, *112*, 9161–9175.
- (9) Miller, R. J. D. *Annu. Rev. Phys. Chem.* **1991**, *42*, 581–614.
- (10) Straub, J. E.; Karplus, M. *Chem. Phys.* **1991**, *158*, 221–248.
- (11) Li, H.; Elber, R.; Straub, J. E. *J. Biol. Chem.* **1993**, *268*, 17908–17916.
- (12) Sagnella, D. E.; Straub, J. E. *J. Phys. Chem. B* **2001**, *105*, 7057–7063.
- (13) Bu, L.; Straub, J. E. *J. Phys. Chem. B* **2003**, *107*, 10634–10639.
- (14) Okazaki, I.; Hara, Y.; Nagaoka, M. *Chem. Phys. Lett.* **2001**, *337*, 151–157.
- (15) Petrich, J. W.; Poyart, C.; Martin, J. L. *Biochemistry* **1988**, *27*, 4049–4060.
- (16) Lian, T.; Locke, B.; Kholodenko, Y.; Hochstrasser, R. M. *J. Phys. Chem.* **1994**, *98*, 11648–11656.
- (17) Zhang, Y.; Fujisaki, H.; Straub, J. E. *J. Phys. Chem. B* **2007**, *111*, 3243–3250.
- (18) Walther, M.; Raicu, V.; Ogilvie, J. P.; Phillips, R.; Kluger, R.; Miller, R. J. D. *J. Phys. Chem. B* **2005**, *109*, 20605–20611.
- (19) Nagy, A. M.; Raicu, V.; Miller, R. J. D. *Biochim. Biophys. Acta* **2005**, *1749*, 148–172.

- (20) Hill, J. R.; Tokmakoff, A.; Peterson, K. A.; Sauter, B.; Zimdars, D.; Dlott, D. D.; Fayer, M. D. *J. Phys. Chem.* **1994**, *98*, 11213–11219.
- (21) Rector, K. D.; Rella, C. W.; Hill, J. R.; Kwok, A. S.; Sligar, S. G.; Chien, E. Y. P.; Dlott, D. D.; Fayer, M. D. *J. Phys. Chem. B* **1997**, *101*, 1468–1475.
- (22) Rector, K. D.; Jiang, J.; Berg, M. A.; Fayer, M. D. *J. Phys. Chem. B* **2001**, *105*, 1081–1092.
- (23) Finkelstein, I. J.; Goj, A.; McClain, B.; Massari, A. M.; Merchant, K. A.; Loring, R. F.; Fayer, M. D. *J. Phys. Chem. B* **2005**, *109*, 16959–16966.
- (24) Xie, A.; van Der Meer, L.; Hoff, W.; Austin, R. H. *Phys. Rev. Lett.* **2000**, *84*, 5435–5438.
- (25) Frauenfelder, H.; McMahon, B. H. *Bio. Syst.* **2001**, *62*, 3–8.
- (26) Elber, R.; Gibson, Q. H. *J. Phys. Chem. B* **2008**, *112*, 6147–6154.
- (27) Mizutani, Y.; Kitagawa, T. *Science* **1997**, *278*, 443–446.
- (28) Mizutani, Y.; Kitagawa, T. *Chem. Rec.* **2001**, *1*, 258–275.
- (29) Kruglik, S. G.; Mojzes, P.; Mizutani, Y.; Kitagawa, T.; Turpin, P.-Y. *J. Phys. Chem. B* **2001**, *105*, 5018–5031.
- (30) Kitagawa, T.; Haruta, N.; Mizutani, Y. *Biopolymers* **2002**, *61*, 207–213.
- (31) Gao, Y.; Koyama, M.; El-Mashtoly, S. F.; Hayashi, T.; Harada, K.; Mizutani, Y.; Kitagawa, T. *Chem. Phys. Lett.* **2006**, *429*, 239–243.
- (32) Koyama, M.; Neya, S.; Mizutani, Y. *Chem. Phys. Lett.* **2006**, *430*, 404–408.
- (33) Shigeto, S.; Dlott, D. D. *Chem. Phys. Lett.* **2007**, *447*, 134–139.
- (34) Zhang, Y.; Straub, J. E. *J. Phys. Chem. B* **2009**, *113*, 825–830.
- (35) Zhang, Y.; Fujisaki, H.; Straub, J. E. *J. Chem. Phys.* **2009**, *130*, 025102.
- (36) Gregurick, S. K.; Chaban, G. M.; Gerber, R. B. *J. Phys. Chem. A* **2002**, *106*, 8696–8707.
- (37) Fujisaki, H.; Stock, G. *J. Chem. Phys.* **2008**, *129*, 134110.
- (38) Decatur, S. M. *Acc. Chem. Res.* **2006**, *39*, 169–175.
- (39) Mukherjee, S.; Chowdhury, P.; Gai, F. *J. Phys. Chem. B* **2007**, *111*, 4596–4602.
- (40) Mukherjee, S.; Chowdhury, P.; Bunagan, M. R.; Gai, F. *J. Phys. Chem. B* **2008**, *112*, 9146–9150.
- (41) Strasfeld, D. B.; Ling, Y. L.; Shim, S.-H.; Zanni, M. T. *J. Am. Chem. Soc.* **2008**, *130*, 6698–6699.
- (42) Davydov, A. S. *Solitons in molecular systems*; D. Reidel Publishing Company: Dordrecht, The Netherlands, 1985.
- (43) Hamm, P.; Lim, M.; Hochstrasser, R. M. *J. Phys. Chem. B* **1998**, *102*, 6123–6138.
- (44) Peterson, K. A.; Rella, C. W.; Engholm, J. R.; Schwettman, H. A. *J. Phys. Chem. B* **1999**, *103*, 557–561.
- (45) Fujisaki, H.; Straub, J. E. *J. Phys. Chem. B* **2007**, *111*, 12017–12023.
- (46) Zanni, M. T.; Asplund, M. C.; Hochstrasser, R. M. *J. Chem. Phys.* **2001**, *114*, 4579–4590.
- (47) Cho, M. *J. Chem. Phys.* **2003**, *118*, 3480–3490.
- (48) Ham, S.; Kim, J.-H.; Lee, H.; Cho, M. *J. Chem. Phys.* **2003**, *118*, 3491–3498.
- (49) Kwac, K.; Cho, M. *J. Chem. Phys.* **2003**, *119*, 2247–2255.
- (50) Kwac, K.; Cho, M. *J. Chem. Phys.* **2003**, *119*, 2256–2263.
- (51) Kaledin, A. L.; Bowman, J. M. *J. Phys. Chem. A* **2007**, *111*, 5593–5598.
- (52) Zhuang, W.; Abramavicius, D.; Hayashi, T.; Mukamel, S. *J. Phys. Chem. B* **2006**, *110*, 3362–3374.
- (53) Hayashi, T.; Mukamel, S. *J. Phys. Chem. B* **2007**, *111*, 11032–11046.
- (54) Rubtsov, I. V.; Wang, J.; Hochstrasser, R. M. *J. Phys. Chem. A* **2003**, *107*, 3384–3396.
- (55) DeCamp, M. F.; DeFlores, L.; McCracken, J. M.; Tokmakoff, A.; Kwac, K.; Cho, M. *J. Phys. Chem. B* **2005**, *109*, 11016–11026.
- (56) Fujisaki, H.; Yagi, K.; Hirao, K.; Straub, J. E. *Chem. Phys. Lett.* **2007**, *443*, 6–11.
- (57) Owrutsky, J. C.; Raftery, D.; Hochstrasser, R. M. *Annu. Rev. Phys. Chem.* **2007**, *45*, 519–555.
- (58) Deflores, L. P.; Ganim, Z.; Ackley, S. F.; Chung, H.; Tokmakoff, A. *J. Phys. Chem. B* **2006**, *110*, 18973–18980.
- (59) Dijkstra, A. G.; Jansen, T. I. C.; Bloem, R.; Knoester, J. *J. Chem. Phys.* **2007**, *127*, 194505.
- (60) Bloem, R.; Dijkstra, A. G.; Jansen, T. I. C.; Knoester, J. *J. Chem. Phys.* **2008**, *129*, 055101.
- (61) Fujisaki, H.; Zhang, Y.; Straub, J. E. *J. Chem. Phys.* **2006**, *124*, 144910.
- (62) Guo, H.; Karplus, M. *J. Phys. Chem.* **1992**, *96*, 7273–7287.
- (63) Guo, H.; Karplus, M. *J. Phys. Chem.* **1994**, *98*, 7104–7105.
- (64) Han, W.-G.; Suhai, S. *J. Phys. Chem.* **1996**, *100*, 3942–3949.
- (65) Schmidt, J. R.; Corcelli, S. A.; Skinner, J. L. *J. Chem. Phys.* **2004**, *121*, 8887–8896.
- (66) Pu, L.; Wang, Q.; Zhang, Y.; Miao, Q.; Kim, Y.; Zhang, Z. *Adv. Quantum Chem.* **2008**, *54*, 271–295.
- (67) Kubelka, J.; Keiderling, T. A. *J. Phys. Chem. A* **2001**, *105*, 10922–10928.
- (68) Frisch, M. J.; Trucks, G. W.; Schlegel, H. B.; Scuseria, G. E.; Robb, M. A.; Cheeseman, J. R.; Montgomery, J. A., Jr.; Vreven, T.; Kudin, K. N.; Burant, J. C.; Millam, J. M.; Iyengar, S. S.; Tomasi, J.; Barone, V.; Mennucci, B.; Cossi, M.; Scalmani, G.; Rega, N.; Petersson, G. A.; Nakatsuji, H.; Hada, M.; Ehara, M.; Toyota, K.; Fukuda, R.; Hasegawa, J.; Ishida, M.; Nakajima, T.; Honda, Y.; Kitao, O.; Nakai, H.; Klene, M.; Li, X.; Knox, J. E.; Hratchian, H. P.; Cross, J. B.; Bakken, V.; Adamo, C.; Jaramillo, J.; Gomperts, R.; Stratmann, R. E.; Yazyev, O.; Austin, A. J.; Cammi, R.; Pomelli, C.; Ochterski, J. W.; Ayala, P. Y.; Morokuma, K.; Voth, G. A.; Salvador, P.; Dannenberg, J. J.; Zakrzewski, V. G.; Dapprich, S.; Daniels, A. D.; Strain, M. C.; Farkas, O.; Malick, D. K.; Rabuck, A. D.; Raghavachari, K.; Foresman, J. B.; Ortiz, J. V.; Cui, Q.; Baboul, A. G.; Clifford, S.; Cioslowski, J.; Stefanov, B. B.; Liu, G.; Liashenko, A.; Piskorz, P.; Komaromi, I.; Martin, R. L.; Fox, D. J.; Keith, T.; Al-Laham, M. A.; Peng, C. Y.; Nanayakkara, A.; Challacombe, M.; Gill, P. M. W.; Johnson, B.; Chen, W.; Wong, M. W.; Gonzalez, C.; Pople, J. A. *Gaussian 03*, revision C.02; Gaussian, Inc.: Wallingford, CT, 2004.
- (69) Fujisaki, H.; Bu, L.; Straub, J. E. *Adv. Chem. Phys.* **2005**, *130*, 179–203.
- (70) Kitano, M.; Fukuyama, T.; Kuchitsu, K. *Bull. Chem. Soc. Jpn.* **1973**, *46*, 384–387.
- (71) Brooks, B. R.; Bruccoleri, R. E.; Olafson, B. D.; States, D. J.; Swaminathan, S.; Karplus, M. *J. Comput. Chem.* **1983**, *4*, 187–217.
- (72) Pulay, P.; Fogarasi, G.; Pang, F.; Boggs, J. E. *J. Am. Chem. Soc.* **1979**, *101*, 2550–2560.
- (73) Mayne, L.; Hudson, B. *J. Phys. Chem.* **1991**, *95*, 2962–2967.
- (74) Chen, X. G.; Schweitzer-Stenner, R.; Asher, S. A.; Mirkin, N.; Krimm, S. *J. Phys. Chem.* **1995**, *99*, 3074–3083.
- (75) Zhang, Y.; Straub, J. E. *J. Chem. Phys.*, in press.
- (76) Zhang, Y.; Straub, J. E. *J. Chem. Phys.*, submitted.
- (77) Agbo, J. K.; Leitner, D. M.; Evans, D. A.; Wales, D. J. *J. Chem. Phys.* **2005**, *123*, 124304.
- (78) Sagnella, D. E.; Straub, J. E. *Biophys. J.* **1999**, *77*, 70–84.